Headgroup Immersion Depth and Its Effect on the Lateral Diffusion of Amphiphiles at the Air/Water Interface

Young Soo Kang[†] and Marcin Majda*

Department of Chemistry, University of California at Berkeley, Berkeley, California 94720-1460

Received: October 6, 1999; In Final Form: December 2, 1999

Two-dimensional electrochemical measurements were carried out with line microelectrodes positioned in the plane of the air/water interface to characterize the lateral mobilities of several long alkyl chain ferrocene amphiphiles possessing headgroups of different polarity. In the liquid range of mean molecular areas (MMA) of 55−95 Å^2/molecule, the diffusion constants increase linearly with MMA. The slopes of these linear plots depend strongly on the headgroup polarity, demonstrating that the immersion depth of the amphiphiles is the key factor in determining their lateral mobility. Investigations of the alkane chain length dependence revealed an unusual inverse effect on *D*. This suggests that for this class of amphiphiles the immersion depth depends not only on the headgroup polarity but also on the length of chains. Thus, the longer alkane chain amphiphiles exhibit smaller immersion depth and larger diffusion constants of lateral mobility. The effects of the immersion depth and chain length were analyzed in terms of a modified hydrodynamic model of Saffman and Delbrück. Quantitative analysis of the experimental data yielded the average values of the headgroup immersion depth for the dodecane- and hexadecaneferrocenecarboxamides of 6.4 and 4.0 Å, respectively.

Introduction

Lateral diffusion of lipids in bilayer assemblies was first recognized and measured by Devaux and McConnell[1] and by Träuble and Sackmann[2] using electron spin resonance (ESR) methods. Mobility of lipids at the air/water interface has been a subject of considerable interest,[3−7] reflecting the importance of this class of quasi-two-dimensional (2D) assemblies and their dynamical properties as model systems of biological membranes.[8−11] Fluorescence recovery after photobleaching (FRAP) has been used predominantly in these studies,[3] but other fluorescence techniques are also known.[6] Several reviews describing experimental techniques and results concerning lipid lateral diffusion in artificial and natural systems are available in the literature.[12−15] Also available are descriptions and critical evaluations of the theoretical models used to treat lateral lipid diffusion.[14,15] Briefly, two theoretical approaches seem to dominate: a hydrodynamic theory of Saffman and Delbrück,[16,17] later extended by Hughes and co-workers,[18] and a free-volume theory of Cohen and Turnbull,[19,20] adopted to 2D membrane diffusion by Galla et al.[21] As we show below, neither model is capable of accounting fully for the role of the headgroup interactions with the aqueous subphase in the lateral diffusion of lipids.

In this paper, we describe a set of electrochemical experiments investigating lateral diffusion of several long alkyl chain amphiphilic ferrocene derivatives. We focus on the dependence of the lateral mobility on the length of the alkyl chains and on the polarity of the headgroups. In our electrochemical approach, we take advantage of "line" microelectrodes, which can be positioned in the plane of the air/water interface and which address electrochemically active species forming Langmuir monolayers at that interface.[22,23] As shown schematically in Figure 1, a 900-Å-thick microelectrode is immersed in the aqueous subphase. The wettability of the microband is limited by a monolayer of octadecanethiol which is self-assembled on the front face of gold. This defines the 2D character of the electrode in the measurements involving electrochemically active species confined to the air/water interface (see also the Experimental Section). The principle of the measurement is analogous to that employed in FRAP.[23] By controlling the potential of the line microelectrode, one is capable of setting a concentration gradient of the redox species within the monolayer and of monitoring the time evolution of the current due to oxidation or reduction of the amphiphilic molecules. The latter is proportional to the lateral, diffusive rate of arrival of the amphiphilic species to the line electrode. Specifically, in the case of the alkylferrocenecarboxamide amphiphiles (C_nFc), the electrochemical reaction in question is a simple, reversible one-electron oxidation of the ferrocene group: $C_nFc - 1e^- \leftrightarrow C_nFc^+$. As shown previously, if the experiments are carried out on a perchloric acid subphase, the amphiphilic ferricinium cation becomes ion paired with ClO_4^- ions and is both chemically stable and water insoluble.[22]

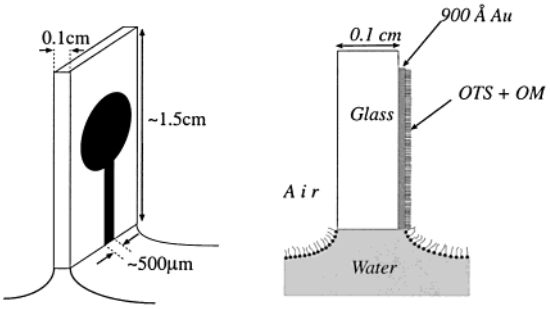

Figure 1. Schematic design of a line microelectrode and its positioning at the air/water interface. Half of the initially produced electrode substrate is shown. (See the Experimental Section for details.)

The electrochemical measurements can be done either in

* Corresponding author. E-mail: majda@socrates.berkeley.edu.
[†] Permanent address: Department of Chemistry, Pukyong National University, NamGu, Pusan 608-737, Korea.

10.1021/jp993566m CCC: $19.00
Published on Web 02/08/2000

cyclic voltammetric (potential sweep) or chronoamperometric (potential step) modes, on the time scale from ca. 1 to 1000 ms. The diffusion constants obtained from such experiments ($10^{-7}-10^{-6}$ cm^2/s) are invariant over this time range.[22] The latter corresponds to diffusion layer thicknesses (δ) in the range of 0.1−10 μm ($\delta \cong \sqrt{2Dt}$). This demonstrates that the lateral mobility of the C_nFc species is unaffected by the growing population of the ferrocenium ($C_nFc^+ClO_4^-$) species in the diffusion layer expanding against the line microelectrode. These measurements report macroscopic (long-range) diffusion constants of the amphiphilic ferrocene molecules in their quasi-2D monolayers at that interface.

In this paper, we first address the issue of the chain-length dependence of the lateral diffusion coefficient for a series of alkylferrocenecarboxamides. These measurements produced an unexpected result: *the amphiphiles with shorter alkyl chains diffuse slower than those with longer alkyl chains*. This surprising finding led us to investigate the effect of the immersion depth of polar headgroups on the surfactants' lateral mobility. The latter is related to the headgroup polarity. We have adopted a hydrodynamic model of Saffman and Delbrück[16] to interpret our data. We conclude that viscous coupling of the headgroups to a subphase (strongly related to headgroup polarity) is the key factor determining the magnitude of the lateral diffusion constants of these surfactants in the entire liquid range of surface concentrations. To explain the counterintuitive chain-length dependence of the C_nFc mobilities found here, we postulate that the immersion depth of the alkylferrocenecarboxamides is modified by the van der Waals interactions within the hydrocarbon region: stronger interactions between hydrocarbon chains of a longer chain derivative lead to a shallower immersion of its headgroup and result in its greater lateral mobility. Fitting the experimental data to the hydrodynamic model allowed us to assess the variations in the headgroup immersion depth as a function of the chain length.

Experimental Section

Materials. *N*-Alkylferrocenecarboxamides (C_nFc with n = 12, 14, 16) were synthesized and purified according to the previously used procedures.[22] The synthesis, purification, and characterization of the three other long alkane chain ferrocene amphiphiles were described previously.[24] Briefly, undecylferrocene ketone [Fc−CO−$(CH_2)_{11}$−H] was synthesized by the Friedel−Craft acylation of ferrocene with lauroyl chloride in methylene chloride. Synthesis of undecylferrocenealcohol [Fc−COH−$(CH_2)_{11}$−H] was carried out by reduction of undecylferrocene ketone with $NaBH_4$ in methanol. Dodecylferrocene ester [Fc−CO−O−$(CH_2)_{12}$−H] was synthesized by reacting ferroceneacyl chloride with dodecyl alcohol in anhydrous THF in the presence of pyridine. The products were purified repeatedly by column chromatography (silica gel, eluted with 20:1 *n*-hexane/ethyl acetate or, for the ester derivative, 10:1 *n*-hexane/ethyl ether) and characterized by TLC, proton NMR, and elemental analysis.[24]

House-distilled H_2O was passed through a four-cartridge Barnstead Nanopure II purification train consisting of Macropure pretreatment, Organics Free for removing trace organics, two ion exchangers, and a 0.2 mm hollow-fiber final filter for removing particles. Its resistivity was 18.3 MΩ cm. Octadecyltrichlorosilane (OTS) and (3-mercaptopropyl)trimethoxysilane (MPS) were from Petrarch Systems Inc. OTS was vacuum-distilled into sealed glass ampules, which were opened as needed immediately prior to the individual experiments. Octadecylmercaptan (OM; Tokyo Kasei, Tokyo, Japan) and octadecanol (Aldrich) were used without further purification. Reagent-grade 70% $HClO_4$ (Aldrich), chloroform (Fisher, ACS certified spectranalyzed), methanol (Fisher, spectroscopic grade), glycerol (Fisher, ACS certified spectranalyzed), and all of the other reagents were used as received.

Monolayer Techniques. The general experimental setup used in 2D electrochemical measurements on the air/water interface was described recently.[25] A KSV model 2200 Langmuir trough (45 × 15 cm^2) was thermostated at 26 °C. It was equipped with a surface pressure Wilhelmy plate microbalance. Filter paper was used as the Wilhelmy plate. All experiments involving the Langmuir trough were done in inert gas enclosures. With the exception of the brief period of time during recording of the 2D voltammograms, the box was continuously purged with filtered (0.01 μm Metheson membrane gas filter) nitrogen. The relative humidity in the box was kept at 25−30%. A more detailed protocol of the Langmuir experiments has been described previously.[25] Surface tension measurements of the glycerol solutions were done with a DuNouy tensiometer (model 70535, CSC Scientific Co. Inc.). Their viscosities (at 26 °C) were measured with an Ostwald viscometer against distilled water.

Fabrication of the Line Microband Electrodes. Electrochemical measurements at the air/water interface required specially designed line microelectrodes that can be positioned in the plane of the air/water interface. The details of their fabrication procedure have been described previously.[22] Briefly, these electrodes are produced by creating a sharp gradient of wettability along a fracture line of 900−1050 Å thick gold films, vapor-deposited on microscope glass slides (ca. 8 × 20 mm^2). The pattern of the initially deposited gold film (see Figure 1) includes two circular areas, later used as electrical contact pads, and a strip of gold (0.5 mm in width) running between them. Following gold vapor deposition, monolayers of octadecane mercaptan (from 0.40 mM solution in 80:20 (v:v) ethanol/water) and octadecyltrichlorosilane (from a 2% solution in a 10:1:1 mixture of *n*-hexadecane, chloroform, and carbon tetrachloride under an argon atmosphere) are formed on gold and on glass surfaces, respectively, by self-assembly. This renders all of the surfaces of the substrate hydrophobic. By breaking such an electrode substrate in half (along a line drawn with a diamond pencil on the reverse side of the glass substrate perpendicular to the gold strip), one exposes a clean, and thus hydrophilic, edge surface of glass and gold and creates two identical microelectrodes. The newly exposed edge of gold forms a microband electrode ca. 900 Å in width. The length of the microband (0.5 mm) is determined by the width of the vapor-deposited gold strip. These microelectrodes are positioned at the air/water interface by touching the water surface with the clean, hydrophilic edge of the electrode substrate. Thus, a line of wettability is formed along the edge of the gold microband between the hydrophilic gold cross-sectional area and the hydrophobic (OM-coated) front face of the gold strip. This line of wettability defines the line microelectrode which contacts the molecules spread at the air/water interface.

Electrochemical Experiments. Cyclic voltammetry was performed with an Ensman model 852 bipotentiostat (Bloomington, IN) in a three-electrode configuration under computer control. The reference electrode (SCE or a quasi-reference, Ag wire) and the Pt counter electrode were immersed in the subphase in a Langmuir trough behind the barrier, where their presence did not interfere with a monolayer compression. The line electrodes were positioned at the air/water interface, following monolayer spreading and solvent evaporation (typi-

cally at 120 Å^2/molecule) but before initiation of monolayer compression. Under these conditions, the value of the capacitive current recorded at 0.2 V/s constituted the final criterion of an electrode quality. Acceptable values were in the range 0.05−0.1 nA. Those line electrodes that exhibited an initial charging current in excess of 0.5 nA were discarded immediately. Performance of the line electrodes at the air/water interface was reproducible for ca. 30−60 min. Subsequent slow contamination of the microband leads to a decrease of measured currents, and the electrode must then be discarded. In the range of mean molecular areas (MMAs) of 120−100 Å^2/molecule, due to the two-phase (G/L) coexistence state of the monolayers, the 2D voltammograms were irreproducible and were therefore not recorded in routine experiments. At lower MMAs, monolayers were compressed at 8 Å^2 molecule^{-1} min^{-1}, in steps of 4 Å^2/molecule. Following each compression step and a 10 s equilibration time, two consecutive current−voltage curves were recorded and a next compression step was activated.

Least-Squares Minimization Routine. Fitting of the hydrodynamic equation (eq 3) to the experimental data was done with Matlab software using the multivariable minimization algorithm (fmins) based on a simplex search method.[26] To avoid erroneous selection of a local minimum, each minimization run was tested with several sets of different starting values. These were randomly varied within ca. 1 order of magnitude around the final converged values.

Results and Discussion

Chain Length Effect on the Lateral Mobility. In our previous reports,[22,23] the dependence of the lateral diffusion constant (D) on the surface concentration of the alkane derivatives of ferrocenecarboxamide was analyzed in terms of the free-area theory of Cohen and Turnbull.[19] We have also used the Enskog kinetic theory of dense gases,[27] extended by Alder and co-workers to liquid densities with their molecular dynamics calculations of a hard-sphere liquid.[28] The latter theory proved useful in that it allowed us to interpret the experimentally obtained linear dependence of D on the MMA of the amphiphiles on the water surface (A) or on its relative area, A/A_0.[23] Specifically, Alder's hard-sphere diffusion constant (D_{HS}) is expressed by

$$D_{HS} = \frac{\sigma}{4}\left(\frac{\pi RT}{m}\right)^{1/2}(Z-1)^{-1}\left(\frac{D_{HS}}{D_E}\right) \qquad (1)$$

where σ is the molecular diameter, m is molecular mass, and Z is the compressibility factor ($Z = PV/RT$). For the hard-sphere liquids, Z can be related to the relative volume of the fluid V/V_0 (V is the actual volume of the fluid and V_0 is the volume occupied by hard spheres when they are close packed). The term (D_{HS}/D_E) is the correction of the Enskog diffusion constant (D_E) obtained by Alder et al. as a function of V/V_0, from their molecular dynamics calculations.[28] As shown in Figure 2A, eq 1 gives a linear plot of D_{HS} vs V/V_0. When the molecular mass of C_{16}Fc (397 g/mol) is used, a slope of 9.56×10^{-5} cm^2/s is obtained. Figure 2B shows an analogous plot (D vs relative free area, A/A_0, with $A_0 = 47$ Å^2/molecule) obtained with the experimental data for C_{16}Fc. In view of the quasi-2D character of our monolayer films, the comparison made here between 3D hard-sphere simulations and our system is appropriate to within a small constant factor relating the different dimensionalities of these two cases.

There are two conspicuous differences between the theoretical prediction and the experimental results. First, the hard-sphere theory predicts that fluids freeze when their relative free volume decreases below 0.5 (see Figure 2A).[28] Our data do not reflect that prediction. Measurable values of the lateral diffusion coefficient can be obtained at significantly higher 2D densities, as is evident from the data for $A_f/A_0 < 0.5$ in Figure 2B. The second difference pertains to the magnitude of the slope of the plots in Figure 2. The slope of the experimental data in Figure 2B equal to 1.22×10^{-6} cm^2/s corresponds to an apparent molecular weight of C_{16}Fc that is ca. 6.1×10^3 times larger than its actual value. One can rationalize these differences in view of the physical differences existing between hard spheres and our C_{16}Fc molecules at the air/water interface. Specifically, the extent of lateral interactions in the latter case is likely to be larger because of some chain−chain entanglement. Such entanglement would result in a lower mobility of C_{16}Fc relative to hard spheres of the same mass. In addition, headgroup immersion and a resulting viscous coupling to the aqueous subphase is a substantial factor which will also result in slower lateral mobility.

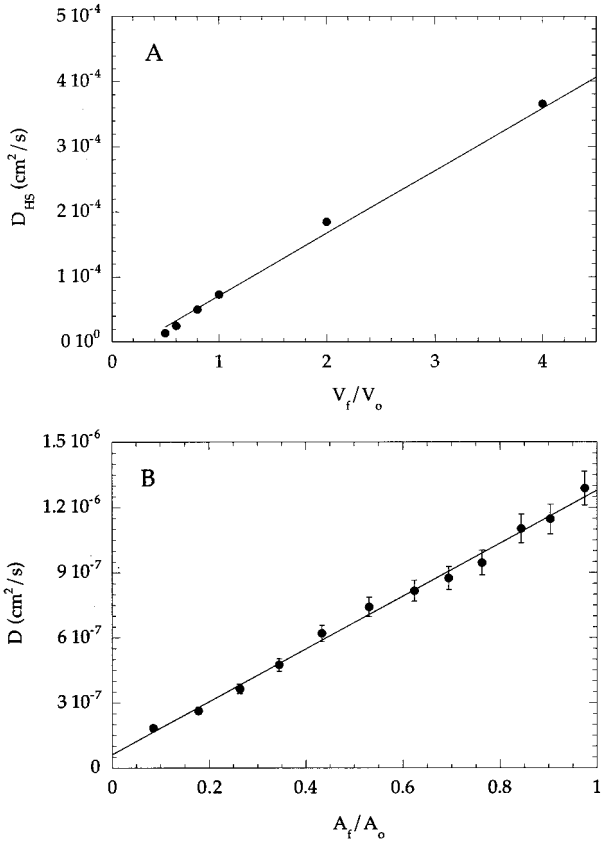

Figure 2. (A) Plot of D vs V_f/V_0 according to the Enskog−Alder theory of dense gases (see eq 1) obtained with the molecular mass of C_{16}Fc (397 g/mol). (B) Analogous plot of the experimentally obtained values of D for C_{16}Fc at the air/water interface vs A_f/A_0.

To address these issues, we first made measurements investigating the chain-length dependence. We synthesized three ferrocenecarboxamide derivatives with 12, 14, and 16 carbon atoms in the alkyl chains and measured their lateral mobilities. All measurements were carried out on a $HClO_4$ subphase (0.05−1.0 M). The pressure vs area (π−A) isotherms of the C_{12}Fc and C_{16}Fc derivatives are shown in Figure 3. Within experimental error (ca ±5%), all three derivatives exhibit indistinguishable π−A isotherms. The liquid region of these monolayers extends from ca. 95 to 35 Å^2/molecule and can be characterized by an apparent MMA of 50 (±3) Å^2/molecule when the most incompressible region of the π−A isotherms is extrapolated to

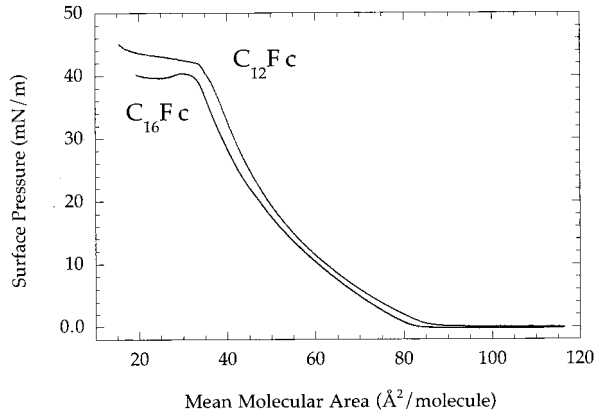

Figure 3. Surface pressure−MMA isotherms for $C_{16}Fc$ and $C_{12}Fc$ on 1 M $HClO_4$ at 26 °C.

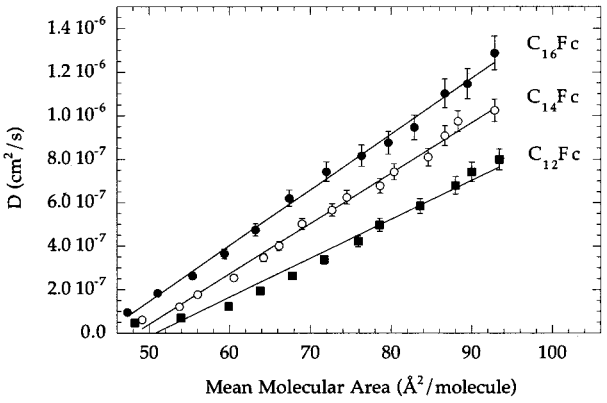

Figure 4. Plots of the *D* values for $C_{16}Fc$, $C_{14}Fc$, and $C_{12}Fc$ vs MMA obtained voltammetrically at the air/water interface (1 M $HClO_4$) at 26 °C.

$\pi = 0$. Further compression (not shown) leads to a second incompressible region which yields a limiting MMA of 20 (±2) Å²/molecule following extrapolation to $\pi = 0$. Thus, the hard-sphere interactions of the C_nFc molecules in the liquid region are due to the large ferrocenecarboxamide headgroups.

Similar to the behavior summarized in our previous report, the 2D electrochemistry of the ferrocenecarboxamides showed well-behaved, reversible voltammograms with a monotonically decreasing current as a function of decreasing MMA. The 2D electrochemical measurements were collected in the range of 95−55 Å²/molecule, or below ca. 12 mN/m. The measurements become irreproducible at higher pressures as a result of monolayer collapse at the microband electrodes. The values of the lateral diffusion constants vs MMA obtained from the voltammetric peak currents (averages of three series of measurements done with different monolayers) are plotted in Figure 4.

Unexpectedly, the observed chain-length dependence contradicts both the predictions of the Enskog−Alder theory and the postulate of chain−chain entanglement mentioned above. Clearly, the longer chain derivatives diffuse faster than those with the shorter chains. This counterintuitive chain-length dependence suggests that there exist factors other than lateral interactions which are affecting the mobilities of these amphiphiles.

Effect of Headgroup Polarity on Lateral Mobility. Viscous (hydrodynamic) coupling between lipid monolayers and the subphases on which they were spread has been demonstrated experimentally by canal surface viscometry and fluorescence microscopy.[29−32] While the effect of headgroup hydration has been considered as a factor influencing the lateral mobility of

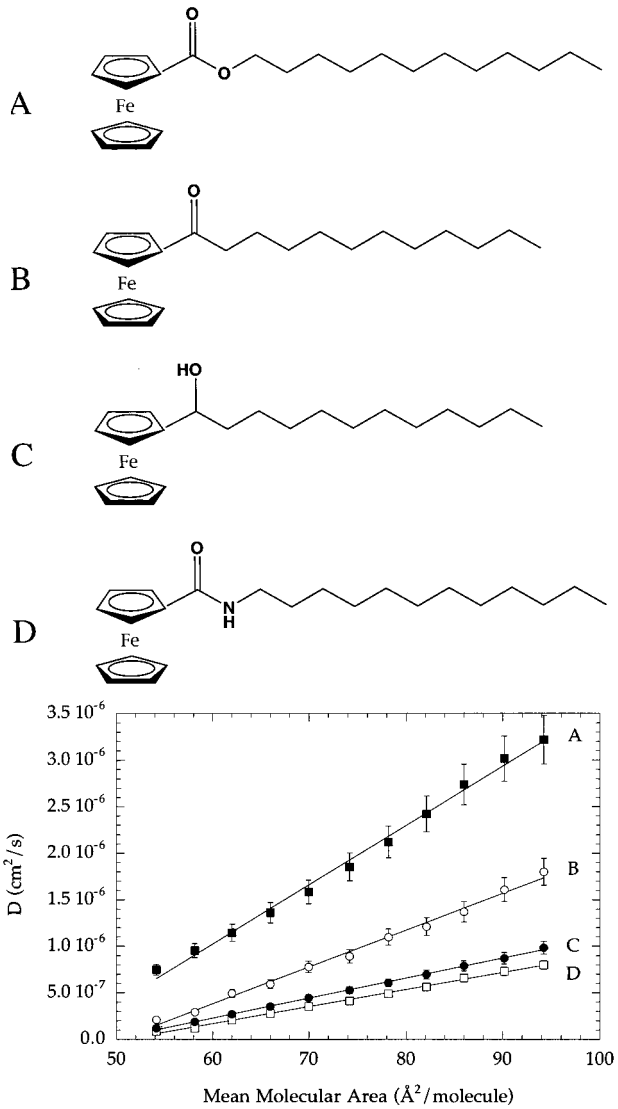

Figure 5. Structures of four ferrocene amphiphiles of different headgroup polarities and the corresponding plots of their lateral diffusion constants vs MMA obtained electrochemically on the water surface (1 M $HClO_4$) at 26 °C.

phospholipids in their bilayer assemblies in the framework of the free-area theory,[33] the effect of headgroup polarity has never been studied systematically. To address this issue, we synthesized four ferrocene derivatives with nearly equal chain lengths but with different polar groups next to ferrocene. Their structures are shown in Figure 5, together with their lateral diffusion data obtained voltammetrically under the same conditions as those in Figure 4. The strong inverse dependence of the diffusion constant on the headgroup polarity is the main feature of this data set. This shows that at any surface concentration coupling of the polar headgroups to the subphase, a medium of a relatively high viscosity, bears a substantial effect on the surfactants' mobility. Consequently, the ester derivative which has the least polar headgroup diffuses faster than all of the other ferrocene derivatives with more polar headgroups.

To probe this effect further, we carried out lateral diffusion measurements of two ferrocenecarboxamides ($C_{12}Fc$ and $C_{16}Fc$) on the perchloric acid subphases, with increasing viscosity adjusted by addition of glycerol. The latter is known to affect only the bulk water viscosity. It does not partition to the interface. We determined that the surface tension of a 40 wt % glycerol solution (the highest used in our experiments) is only

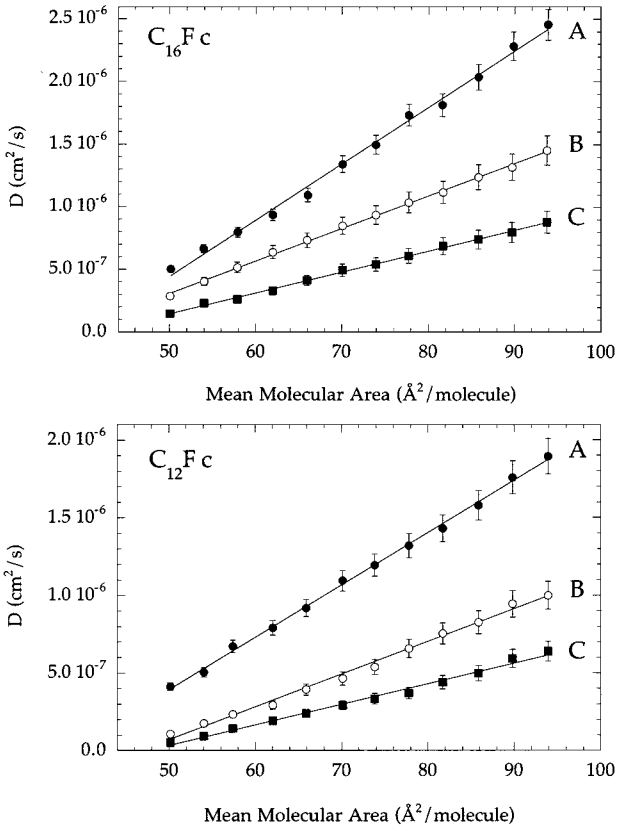

Figure 6. Plots of the lateral D values of $C_{16}Fc$ and $C_{12}Fc$ vs MMA measured on the 0.05 M $HClO_4$ subphases containing (A) 0, (B) 20, and (C) 40 wt % glycerol. The viscosities of these solutions were 1.1, 1.9, and 3.7 cP, respectively.

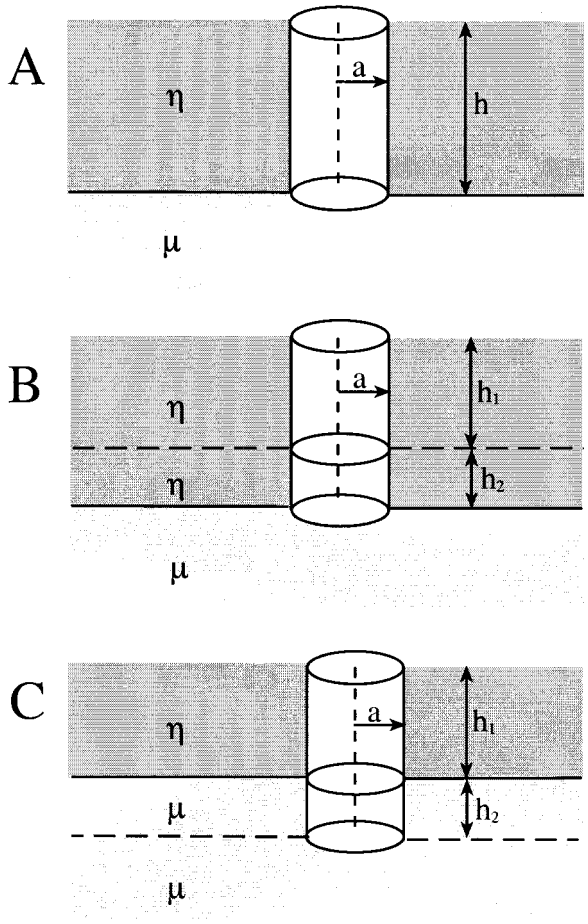

Figure 7. Schematic depiction of cylindrical particle diffusion at the interface of two media of different viscosities. Part A corresponds to the Saffman and Delbrück theory (eq 2). Part C represents our extension of the theory and corresponds to eq 3.

3% higher than that of pure water. The data in Figure 6 show that an increase of the subphase viscosity from 1.06 to 1.87 to 3.06 cP leads indeed to a decrease of the diffusion constants, asserting the significance of the viscous coupling. This effect accounts for the large difference between the observed diffusion constants of these amphiphiles and the predictions of the hard-sphere theory shown in Figure 3.

We also regard the viscous coupling as the effect that accounts for the unusual and counterintuitive chain-length dependence observed in Figures 4 and 6. We postulate that, at least for this group of amphiphiles, their immersion depth is not only a function of the headgroup polarity but that it also depends weakly and inversely on the length of the hydrocarbon chains. To rationalize this postulate, one must consider the energetics of an assembly of amphiphiles at the air/water interface. The total free energy of the system consists of two terms representing the chain−chain interactions and the headgroup hydration. We maintain that in some systems (see discussion below) the total free energy of the system is lowered by decreasing the average immersion depth of the headgroups. The resulting loss of free energy of hydration is surpassed by a gain in the free energy of van der Waals attraction between the more shallowly immersed amphiphiles.

Hydrodynamic Theory of the Lateral Diffusion. To consider these postulates more quantitatively, we make use of a hydrodynamic model formulated by Saffman and Delbrück.[16,17] The model describes quasi-2D translational diffusion of molecules in lipid membranes. The key features of the model are presented in Figure 7A. A diffusing probe species is modeled as a cylinder of radius a and height h embedded in a membrane of thickness h and viscosity η. The membrane, treated as a viscous continuum, is itself positioned between two fluids of viscosity μ_1 and μ_2 (in Figure 7, a monolayer film at the air/water interface is represented and thus $\mu_2 = 0$) representing the aqueous solution bathing the membrane or contacting a Langmuir film. Because translational motion in 2D is always correlated, there is, strictly speaking, no solution to a diffusion problem in true 2D systems.[34] To overcome this problem, Saffman and Delbrück took into account the viscosity of the contacting fluid and imposed a no-slip boundary condition on the cross section of the cylinder. They obtained an expression for a diffusion constant that was later rederived by Hughes et al. to broaden its applicability:[18]

$$D = \frac{kT}{4\pi\eta h}\left[\ln\frac{2}{\epsilon} - \gamma + \frac{4\epsilon}{\pi} - \left(\frac{\epsilon^2}{2}\right)\ln\frac{2}{\epsilon}\right] \qquad (2)$$

Here $\epsilon = \mu a/\eta h$, and γ is Euler's constant. Hughes and co-workers showed that eq 2 is valid for $\epsilon \leq 1$. Hughes and co-workers used the extended theory to model protein and lipid lateral mobility in membranes.[35] In the latter case, they observed that higher than bulk viscosities of the bathing aqueous phase must be assumed to match the experimental results.

To analyze the effects of headgroup polarity in the diffusion of our ferrocene amphiphiles, we extend the Saffman−Delbrück model here to include the headgroup immersion depth. It is clear that eq 2 contains two viscous drag elements affecting the diffusion constant: one acting on the walls of the cylinder (ηh)

and the other acting on the cylinder's base (μa). Thus, we can express the first of the terms as a hypothetical sum $\eta h_1 + \eta h_2$ where $h_1 + h_2 = h$ (see Figure 7B). We can now define h_2 as the headgroup immersion depth. Accordingly, the viscosity of the surrounding medium should be that of the contacting aqueous phase μ (see Figure 7C), and eq 2 becomes

$$D = \frac{kT}{4\pi(\eta h_1 + \mu h_2)}\left[\ln\frac{2}{\epsilon} - \gamma + \frac{4\epsilon}{\pi} - \left(\frac{\epsilon^2}{2}\right)\ln\frac{2}{\epsilon}\right] \quad (3)$$

with $\epsilon = \mu a/(\eta h_1 + \mu h_2)$. It is clear that this modification of the original Saffman equation changes neither its mathematical formalism nor its physical sense. It continues to describe the diffusion constant of a surfactant modeled as a cylinder, in terms of two drag forces. One is acting on the walls of the cylinder immersed partially in the hydrocarbon region of the monolayer (ηh_1) and partially in the aqueous subphase (μh_2). The other is acting on its base through the no-slip boundary condition. The advantage of our modification, as shown below, is the explicit inclusion of the effect of headgroup immersion in the contacting aqueous subphase.

According to eq 3, an isothermal diffusion coefficient of a surfactant is a function of four independent parameters (ηh_1, μ, h_2, and a). Because we are dealing with molecules of known structure and interfacial behavior, we can assume that the radius of the cylinder in the Saffman−Delbrück model is known (a = 4 Å). Here we prefer to use a value consistent with an approximate size of the ferrocene headgroup (on the basis of π−A isotherms) rather than with the radius of the cross section of an alkane chain. Thus, the number of independent variables for a given amphiphile is reduced to three. Using this model, we fit three sets of six experimental values of diffusion constant (D_m) measured at a single MMA (95, 85, and 75 Å^2/molecule) for C_{12}Fc and C_{16}Fc on the subphases of three different bulk viscosities (six data points at each MMA, see Figure 6A,B). This was done by minimizing the sum of squares of the differences (Δ^2) between the six measured and calculated values of D, using a multivariable simplex method as described in the Experimental Section.

$$\Delta^2 = \sum_i (D_{m,i} - D_{c,i})^2 \quad (4)$$

To further decrease the number of independent variables describing this set of data, we made the following simplifying assumptions: (1) We assumed that the product of the hydrocarbon layer viscosity and its thickness (ηh_1) scales with the number of carbon atoms in the alkyl chain. Specifically, ηh_1 represents C_{16}Fc, and the value of this product for C_{12}Fc becomes 0.75 ηh_1. This is reasonable because at constant MMA the density of the hydrocarbon material in the monolayer is approximately invariant with changes of the chain length. (2) The viscosity of the subphase in the headgroup (μ) is likely to be different from its bulk value. However, we assume that it scales with the bulk viscosity. The latter was varied by addition of glycerol. This assumption is supported by the results of Sacchetti and co-workers, who observed a direct correlation between the bulk subphase viscosities (varied with glycerol) and the measured surface area flow rates of a phospholipid monolayer at low surface pressures. Under these conditions the flow rate depends only on the subphase viscosity through viscous coupling.[30] In our experiments, the bulk viscosities are 1.06, 1.87, and 3.06 cP for the conditions featured in Figure 6. Thus, overall the use of eq 3 to fit six measured values of D involves adjustment of four parameters. Two of them (ηh_1 and μ) are common to the entire system, while h_2(C_{12}Fc) and h_2(C_{16}Fc) are specific to the two amphiphiles. Naturally, the use of this model itself is a simplification. As outlined above, it assumes a sharp boundary between the hydrocarbon region, the headgroup region, and the subphase. In reality, it is known that these regions are all substantially diffuse and interpenetrating.[36,37] As a result, the values of the immersion depth and of the other parameters derived from this model should be treated as average quantities of semiquatitative character. However, they are, nevertheless, useful for relative comparisons between analogous systems.

TABLE 1. Comparison of the Measured and Calculated Values of the Lateral Diffusion Constants of C_{16}Fc and C_{12}Fc as a Function of MMA and Subphase Viscosity

		$D \times 10^6$ cm^2/s					
	glycerol[a]	95 Å^2/molecule		85 Å^2/molecule		75 Å^2/molecule	
	(wt %)	exp	calc	exp	calc	exp	calc
C_{16}Fc	0	2.48	2.49	2.04	2.05	1.59	1.61
	20	1.49	1.47	1.23	1.21	0.97	0.95
	40	0.92	0.92	0.75	0.75	0.58	0.59
C_{12}Fc	0	1.92	1.88	1.58	1.53	1.24	1.18
	20	1.02	1.08	0.81	0.88	0.60	0.68*
	40	0.64	0.66	0.51	0.54	0.38	0.42*

[a] The viscosities of the 50 mM $HClO_4$ subphases with 0, 20, and 40 wt % glycerol at 26 °C were 1.06, 1.87, and 3.06 cP, respectively.

TABLE 2. Fit Parameters Obtained from the Hydrodynamic Model (Figure 7C and Eq 3) Characterizing Lateral Diffusion of C_{12}Fc and C_{16}Fc at the Air/Water Interface under Conditions of Figure 6A,B

MMA (Å^2/molecule)	ηh_1 (cP Å)	h_2(C_{16}Fc)[a] (Å)	h_2(C_{12}Fc)[a] (Å)	μ[a] (cP)
95	1.34	4.0	6.4	2.9
85	1.48	4.1	6.4	3.6
75	1.91	4.0	6.5	4.6

[a] The minimization routine (see eq 4 and related discussion) yielded the values of the products: h_2(C_{12}Fc)a, h_2(C_{16}Fc)a, and μa. The values listed above were obtained with an assumption that a = 4 Å.

The results are collected in Tables 1 and 2. We note first that in all cases the results remain within the range of applicability of eq 3. In other words, $\epsilon = \mu a/(\eta h_1 + \mu h_2) \leq 1$. Table 1 lists the measured and calculated values of the diffusion constants. With a couple of exceptions marked with an asterisk, the agreement is well within the experimental precision of the measurements of ca. 5−10%. Table 2 compares the values of ηh_1, μ, h_2(C_{12}Fc), and h_2(C_{16}Fc) obtained for the three selected MMA. The first of these parameters is least significant, because η and h_1 cannot be determined independently. However, its value is certainly reasonable. For example, if we assumed arbitrarily that the average thickness of the C_{16} hydrocarbon layer at 95 Å^2/molecule is $^1/_4$ of the hexadecane chain length (or ca. 5 Å), then its viscosity would be 0.27 cP, a value similar to that of pentane (0.240 cP at 20 °C). The increase of ηh_1 with compression is not unexpected. It reflects a known increase of the liquid hydrocarbon chain length and viscosity with density.

The key fit parameters are the immersion depths, h_2(C_{12}Fc) and h_2(C_{16}Fc). Their absolute magnitudes (6.4 and 4.0 Å, respectively) should be viewed from the perspective of the model and the approximations mentioned above. With this in mind, these values are very reasonable. Both exceed the size of the amide moiety and constitute a fraction of ferrocene's diameter of ca. 8−9 Å. It is interesting to note that they do not vary with the extent of monolayer compression. It is appropriate to examine the role of the bulky ferrocene in this unusual dependence of the immersion depth on the chain length.

Specifically, one might ask, is this a general phenomenon or is it a phenomenon associated only with this class of amphiphiles? We believe that the latter is a more likely answer to this question. In the absence of ferrocene, the dominant tendency of the system to fully hydrate the polar amide group would fix the immersion depth independent of the chain−chain interactions. We postulate that the presence of the large, hydrophobic ferrocene group does not allow the system to fully hydrate the amide group. Therefore, the net free energy of hydration is expected to be less negative and no longer the dominant factor, compared to chain−chain interactions. This, in turn, allows the latter to modulate the immersion depth depending on the chain length, as observed experimentally.

The values of the viscosity of water in the headgroup region are substantially higher than its bulk value. This is reasonable because the interfacial region is in effect a dense aqueous suspension of particles (the headgroups) and as such should be expected to exhibit a higher viscosity than pure water.[38] The increase of μ with the extent of compression (see Table 2) is qualitatively consistent with this fact. Unfortunately, there are no reliable analytical theories that relate the viscosity of a suspension of particles to its density, in this high range of densities. The well-known Einstein formula for the viscosity of a suspension of particles (μ_s), $\mu_s = \mu[1 + \alpha(5/2)]$, where α stands for the ratio of the volumes of particles and pure fluid (V_0/V), is valid for $\alpha \leq 0.02$.[38] Our system exceeds this limit by more than 1 order of magnitude. Consequently, we cannot account for the observed dependence of the lateral diffusion constants on the extent of compression within the framework of this hydrodynamic model. Finally, it is interesting to point out that in all cases analyzed in Tables 1 and 2, the term μh_2 is approximately 1 order of magnitude greater than ηh_1. Therefore, consistent with our measurements (see data in Figures 5 and 6), the viscous coupling of the amphiphiles to the subphase is, in this range of surface concentrations, the predominant source of drag in their lateral mobility. In fact, it is possible to predict that, as the surface concentration of an amphiphile decreases, its lateral mobility should be less and less affected by the chain−chain interactions (ηh_1). At the same time, the water viscosity in the headgroup region, μ, will more accurately reflect the interfacial viscosity of pure water. Ultimately, we expect that the lateral mobility of amphiphiles in monolayers of very low density should be independent of their density and reveal solely the hydrodynamic properties of interfacial water.

Conclusions

We demonstrated that viscous coupling of headgroups to the subphase is the major element determining the lateral mobility of ferrocenecarboxamides at the air/water interface over nearly the entire range of MMAs corresponding to their liquid state. The drag within the hydrocarbon region is the second factor contributing only ca. 10% of the drag (in the MMA range of 75−95 Å^2/molecule). Thus, the lateral mobilities of ferrocene amphiphiles considered in Figures 5 and 6 are cases of self-diffusion restricted by viscous coupling to the aqueous subphase. The immersion depth of these amphiphiles depends strongly on the polarity of their headgroups. Our investigations of the role of chain−chain interactions led also to the discovery of an anomalous dependence of D on the hydrocarbon chain length. These findings were rationalized in view of a modified hydrodynamic theory of Saffman and Delbrück. Quantitative analysis of the D values obtained for ferrocenecarboxamides of two different chain lengths (C_{12} and C_{16}) on subphases of three different bulk viscosities yielded for the first time average values of the product of the C_{16}-hydrocarbon region viscosity and height (ηh_1), the headgroup immersion depths, $h_2(C_{12}Fc)$ and $h_2(C_{16}Fc)$, and an estimate of the subphase viscosity in the headgroup region, μ. These measurements allow us to postulate that mobilities of amphiphiles on the water surface at MMAs in excess of ca. 300 Å^2/molecule should be dominated solely by the polar headgroup drag in the interfacial water and, therefore, become independent of an amphiphile surface concentration. Measurements of lateral mobilities in that range of surface densities should reveal the interfacial viscosity of water.

Acknowledgment. We acknowledge and thank Clayton J. Radke for discussing with us interfacial hydrodynamics and Berni J. Alder for several illuminating discussions of 2D dynamics at the early stages of this project. This research was supported financially by the U.S. National Science Foundation under Grant CHE-9422619.

References and Notes

(1) Devaux, P.; McConnell, H. M. *J. Am. Chem. Soc.* **1972**, *94*, 4475−4481.
(2) Träuble, H.; Sackmann, E. *J. Am. Chem. Soc.* **1972**, *94*, 4499−4510.
(3) Peters, R.; Beck, K. *Proc. Natl. Acad. Sci. U.S.A.* **1983**, *80*, 7183−7187.
(4) Kim, S. H.; Yu, H. *J. Phys. Chem.* **1992**, *96*, 4034−4040.
(5) Tamada, K.; Kim, S. H.; Yu, H. *Langmuir* **1993**, *9*, 1545−1550.
(6) Caruso, F.; Grieser, F.; Thistlethwaite, P. J. *Langmuir* **1993**, *9*, 3142−3148.
(7) Tanaka, K.; Manning, P. A.; Lau, V. K.; Yu, H. *Langmuir* **1999**, *15*, 600−606.
(8) Möhwald, H. *Annu. Rev. Phys. Chem.* **1990**, *41*, 441−476.
(9) Knobler, C. M. Recent Developments in the Study of Monolayers at the Air−Water Interface. In *Advances in Chemical Physics*; Progogine, I., Rice, S., Eds.; John Wiley & Sons: New York, 1990; Vol. 77, pp 397−449.
(10) McConnell, H. M. *Annu. Rev. Phys. Chem.* **1991**, *42*, 171−195.
(11) Knobler, C. M.; Rashmi, C. D. *Annu. Rev. Phys. Chem.* **1992**, *43*, 207−236.
(12) Peters, R. *Cell Biol. Int. Rep.* **1981**, *5*, 733−760.
(13) Wade, C. G. Lateral Diffusion of Lipids. In *Structure and Properties of Cell Membranes*; Benga, G., Ed.; CRC Press: Boca Raton, FL, 1985; Vol. 1, Chapter 4, pp 51−76.
(14) Clegg, R. M.; Vaz, W. L. C. Translational Diffusion of Proteins and Lipids in Artificial Lipid Bilayer Membranes. A Comparison of Experiment with Theory. In *Progress in Protein−Lipid Interactions*; Watts, A., De Pont, J. J. H. H. M., Eds.; Elsevier: Amsterdam, The Netherlands, 1985; Vol. 1, Chapter 5, pp 173−229.
(15) Tocanne, J.-F.; Dupou-Cezanne, L.; Lopez, A. *Prog. Lipid Res.* **1994**, *33*, 203−237.
(16) Saffman, P. G.; Delbrück, M. *Proc. Natl. Acad. Sci. U.S.A.* **1975**, *72*, 3111−3113.
(17) Saffman, P. G. *J. Fluid Mech.* **1976**, *73*, 593−602.
(18) Hughes, B. D.; Pailthorpe, B. A.; White, L. R. *J. Fluid Mech.* **1981**, *110*, 349−372.
(19) Cohen, M. H.; Turnbull, D. *J. Chem. Phys.* **1959**, *31*, 1164−1169.
(20) Turnbull, D.; Cohen, M. H. *J. Chem. Phys.* **1970**, *52*, 3038−3041.
(21) Galla, H. J.; Hartmann, W.; Theilen, U.; Sackmann, E. *J. Membr. Biol.* **1979**, *48*, 215−236.
(22) Charych, D. H.; Landau, E. M.; Majda, M. *J. Am. Chem. Soc.* **1991**, *113*, 3340−3346.
(23) Majda, M. Translational Diffusion and Electron Hopping in Monolayers at the Air/Water Interface. In *Organic Thin Films and Surfaces*; Ulman, A., Ed.; Academic Press: San Diego, 1995; Vol. 20, pp 331−347.
(24) Baydo, R. Lateral Mobility of Long Alkyl Chain Amphiphiles at the Air/Water Interface. M.Sc Thesis, University of California at Berkeley, Berkeley, CA, 1995.
(25) Lee, W.-Y.; Majda, M.; Brezesinski, G.; Wittek, M.; Moebius, D. *J. Phys. Chem. B* **1999**, *103*, 6950−6956.
(26) *Matlab Reference Guide*; The MathWorks Inc.: Natick, MA, 1992.
(27) Tyrrell, H. J. V.; Harris, K. R. *Diffusion in Liquids, A Theoretical and Experimental Study*; Butterworth: London, 1984; Vol. 5, p 266.
(28) Alder, B. J.; Gass, D. M.; Wainwright, T. E. *J. Chem. Phys.* **1970**, *53*, 3813−3826.

(29) Sacchetti, M.; Yu, H.; Zografi, G. *Langmuir* **1993**, *9*, 2168−2171.
(30) Sacchetti, M.; Yu, H.; Zografi, G. *J. Chem. Phys.* **1993**, *99*, 563−566.
(31) Klingler, J. F.; McConnell, H. M. *J. Phys. Chem.* **1993**, *97*, 6096−6100.
(32) Schwartz, D. K.; Knobler, C. M. *Phys. Rev. Lett.* **1994**, *73*, 2841−2844.
(33) Vaz, W. L. C.; Clegg, R. M.; Hallman, D. *Biochemistry* **1985**, *24*, 781−786.
(34) Alder, B. J.; Wainwright, T. E. *Phys. Rev. A* **1970**, *1*, 18−21.
(35) Hughes, B. D.; Pailthorpe, B. A.; White, L. R.; Sawyer, W. H. *Biophys. J.* **1982**, *37*, 673−676.
(36) Lu, J. R.; Hromadova, M.; Simister, E. A.; Thomas, R. K. *J. Phys. Chem.* **1994**, *98*, 11519−11526.
(37) Tarek, M.; Tobias, D. J.; Klein, M. L. *J. Phys. Chem.* **1995**, *99*, 1393−1402.
(38) Lamb, H. *Hydrodynamics*, 6th ed.; Cambridge University Press: Cambridge, U.K., 1932.